Supersolid phases in the bosonic extended Hubbard model

Kwai-Kong Ng and Yung-Chung Chen
Department of Physics, Tunghai University, Taichung 40704, Taiwan
(Received 18 October 2007; revised manuscript received 10 December 2007; published 25 February 2008)

We present a comprehensive numerical study on the ground state phase diagram of the two-dimensional hard core bosonic extended Hubbard model with nearest (V_1) and next nearest neighbor (V_2) repulsions. In addition to the quantum solid and superfluid phases, we report the existence of a striped supersolid and three-quarter (quarter)-filled supersolid at commensurate density $\rho=0.75$ (0.25) due to the interplay of V_1 and V_2 interactions. The nature of the three-quarter-filled supersolid and the associated quantum solid will be discussed. The observed quantum phase transition between the two supersolids of different symmetries is found to be first order.

DOI: 10.1103/PhysRevB.77.052506 PACS number(s): 67.80.kb, 75.10.Jm, 05.30.Jp, 75.40.Mg

The supersolid (SS) state,[1,2] in which both diagonal and off-diagonal long-range order coexist, has been intensively discussed on various models.[3–8] This is partially due to the experimental advance of optical lattices in interacting cold bosonic atoms where the exotic supersolid phase may be observed experimentally. Furthermore, the supersolid phase of spin models is also of great interest as these quantum spin systems may be realized in real materials.[6–8]

The simplest hard core boson model that includes only the nearest neighbor (NN) interaction, however, does not stabilize the supersolid phase on a square lattice.[3–9] To induce the supersolid phase, one may relax the hard core constraint to soft core[4] or include the next nearest neighbor (NNN) interactions.[3] For the latter case, a striped supersolid (SS1) phase is found associated with the half-filled striped solid (QS1) phase, where bosons form stripes that break the x-y symmetry. This stripe structure allows the superfluid component to easily flow through the channels between stripes, and therefore, coexistence of both solid and superfluid ordering is possible. Unlike the striped solid, the hard core checkerboard solid provides no pathway for the superfluid component and no checkerboard SS of hardcore bosons has been found so far, unless NNN hopping is included.[10] In this work, we present a comprehensive study on the phase diagram of the hard core boson Hubbard model with NN and NNN interactions. A three-quarter-filled supersolid that, like the checkerboard SS, preserves the x-y symmetry is stabilized in a large parameter regime of V_1 and V_2. Associated with the supersolid is a three-quarter-filled quantum solid which share the same starlike occupation pattern (see inset of Fig. 1). For clarity, hereafter we refer to this solid and supersolid as the star solid (QS2) and star supersolid (SS2). Interestingly, the supersolids, SS1 and SS2, that possess different underlying symmetries compete in some parameter regimes in which a first order phase transition occurs, in contrast to recent work on a similar model.[10] We tackle the problem with both quantum Monte Carlo (QMC) and variational Monte Carlo (VMC) methods, which give consistent results. A generic Jastrow wave function in the VMC is able to generate the qualitative features of all phases in QMC calculations.

We study the bosonic extended Hubbard model on a two-dimensional square lattice with the Hamiltonian

$$H = -t\sum_{i,j}^{nn}(b_i^\dagger b_j + b_i b_j^\dagger) + V_1\sum_{i,j}^{nn} n_i n_j + V_2\sum_{i,j}^{nnn} n_i n_j - \mu\sum_i n_i, \tag{1}$$

where b ($b^\dagger$) is the boson destruction (creation) operator and Σ^{nn} (Σ^{nnn}) sums over the (next) nearest neighboring sites. To set the energy scale of the problem, we let $t=1$ throughout the Brief Report. At half-filling, the ground state can be a checkerboard solid [with wave vector (π,π)] for strong NN coupling V_1, or a striped solid [with wave vector $(\pi,0)$ or $(0,\pi)$] for strong NNN coupling V_2.[3] For competing values of V_1 and V_2, however, quantum frustration disfavors both solid structures and leads to the condensation of bosons instead, i.e., a superfluid ground state. Upon doping for large V_2, as mentioned above, the striped solid structure provides channels of superflow so that extra bosons can form a superfluid on top of the striped structure which leads to a striped supersolid. Note that the quantum effect eventually drives all

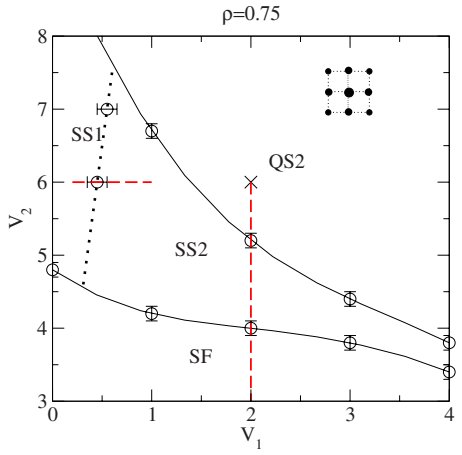

FIG. 1. (Color online) Ground state phase diagram of V_2 as a function of V_1 for density $\rho=0.75$. The first (second) order phase transition is denoted by dotted (solid) lines. The inset shows the boson occupation profile (the star pattern) of the QS2 and SS2 phases. The cross shows a representative point of the QS2 phase at $\rho=0.75$, where the order parameters are plotted in Fig. 2. Lattice sizes of 36×36 and 28×28 are used with temperature $\beta=1/2L$.

bosons to participate in the superflow, although the superfluidity that transverses the stripes is much smaller.[3] For dominating V_1, on the other hand, additional bosons form no condensate on the checkerboard solid because domain formation is energetically more favorable. As a consequence, no supersolid of checkerboard solid ordering is found. The phase diagram at half-filling and the result of doping close to half-filling have been discussed in detail in Ref. 3.

Remarkably, when further increasing doping to $\rho=0.75$, our numerical calculations show a rich phase diagram that contains a superfluid (SF) phase, a star solid phase which has finite structure factor $S(\mathbf{Q})/N=\Sigma_{ij}\langle n_i n_j e^{i\mathbf{Q}\mathbf{r}_{ij}}\rangle/N^2$ at $\mathbf{Q}_0=(\pi,\pi)$, $=(\pi,0)$, and $=(0,\pi)$, and supersolid phases of either star ordering or striped ordering. The result obtained from QMC calculations based on the stochastic series expansion algorithm[11] on a square lattice is presented in Fig. 1. In QMC, the superfluidity, given by $\rho_s=\langle W^2\rangle/4\beta t$, is computed by measuring the winding number fluctuation. The calculation is done by scanning over different μ's grand canonically to search for the right μ that fixes the density at $\rho=0.75$ for each coordinate pair (V_1,V_2) in the diagram. Due to the particle-hole symmetry of the Hamiltonian H, one must obtain the same phase diagram as in Fig. 1 for $\rho=0.25$. In this Brief Reports we will focus on $\rho=0.75$, but all discussion applies to $\rho=0.25$ as well. Let us now discuss each phase in more detail, starting with the star solid QS2.

The inset of Fig. 1 shows the ordering of the QS2. The lattice contains four square sublattices with twice the lattice constant. It is important to stress that QS2 is not a solid, with three fully occupied sublattices and one empty sublattice, which naturally gives $\rho=0.75$. Our calculation shows that all sites have finite occupations as shown in the figure. Owing to the x-y symmetry, two of the sublattices are identical. A typical structure of QS2 has one of the sublattices almost fully occupied, the two identical sublattices have occupation n, while the last sublattice has occupation $\sim 2(1-n)$. For instance, at $V_1=2.0$ and $V_2=6.0$, the occupations on different sublattices are 0.99, 0.37, 0.37, and 0.27, respectively. It is not surprising that quantum fluctuation and the gain in kinetic energy favor this structure rather than the one with one sublattice unoccupied. One important feature of the QS2 phase is that although the $S(\mathbf{Q}_0)/N$ are finite, they are rather small compared to those of the striped solid QS1. In Fig. 2, we show the order parameters as a function of μ at $V_1=2$ and $V_2=6$, a representative point (the cross in Fig. 1) of the SS2 phase in the phase diagram.

A clear plateau appearing in the density curve signals the existence of a solid phase, in which the superfluid density $\rho_{x(y)}$ vanishes, but $S(\mathbf{Q}_0)/N$ (Fig. 2) is finite and remains flat throughout the QS2 phase. Structure factors of all other wave vectors are essentially zero except $S(\mathbf{Q}_0)/N$, which remains finite under finite-size analysis. It is noted that the striped solid QS1 at half-filling has $S(\pi,0)/N\sim 0.2$ (not shown). The small value of $S(\mathbf{Q}_0)/N$ in QS2, therefore, indicates that the solid QS2 is rather *soft*.

Moving away from density $\rho=0.75$ by increasing or reducing μ, there exist supersolid phases (SS2) characterized by the same star solid ordering (wave vector $\mathbf{Q}_0$) as the QS2. In this phase, x-y symmetry is preserved such that

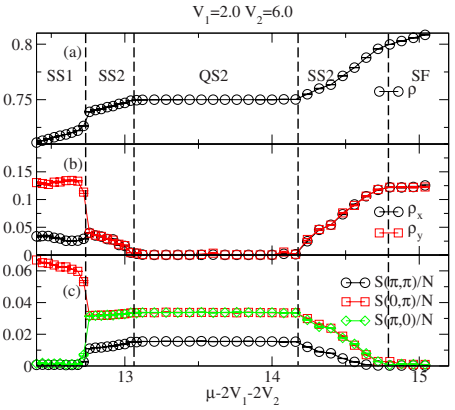

FIG. 2. (Color online) QMC result of (a) boson density ρ, (b) superfluidity ρ_x and ρ_y, and (c) structure factor of wave vectors (π,π), $(0,\pi)$, and $(\pi,0)$, as functions of chemical potential $\mu-2V_1-2V_2$. $V_1=2.0$, $V_2=6.0$, and lattice size is 28×28.

$S(\pi,0)/N=S(0,\pi)/N$ and is about twice $S(\pi,\pi)$. At larger μ, all these peaks reduce simultaneously away from the QS2 and vanish at the same critical point where SF emerges. This implies that SS2 is a unique phase characterized by wave vectors $\mathbf{Q}_0$, but is not a mixture of striped phases. Remarkably, like the QS2 state, the SS2 state has one sublattice being almost fully occupied. Nevertheless, the condensate density $n_{k=0}$ is found to be nonzero in that sublattice. The transition from QS2 to SS2 is second order as both $\rho_{x(y)}$ and $S(\mathbf{Q}_0)/N$ change continuously across phase boundaries and no abrupt change in order parameters is observed. The finite-size effect will change the phase boundaries slightly, but not the general features of the transitions. An example of finite-size scaling of the order parameter in the SS2 phase is demonstrated in Fig. 3.

On the other hand, there is clearly a first order phase transition from SS2 to SS1 where all parameters exhibit a sudden jump at $\mu-2V_1-2V_2\approx 12.72$ as shown in Fig. 2. This discontinuity arises from the distinct broken crystal symmetry of the two supersolids. Our VMC calculation, presented later, also supports the discontinuous phase transition. It is worth noting that a recent study by Chen *et al.*[10] on the

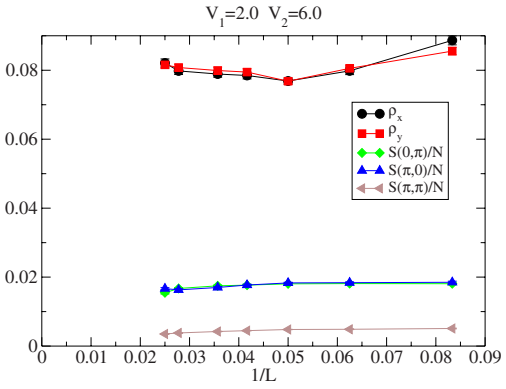

FIG. 3. (Color online) Finite-size scaling of QMC data for ρ_x, ρ_y, $S(0,\pi)/N$, $S(\pi,0)/N$, and $S(\pi,\pi)/N$ of the SS2 phase with $V_1=2.0$, $V_2=6.0$, and $\mu-2V_1-2V_2=14.5$.

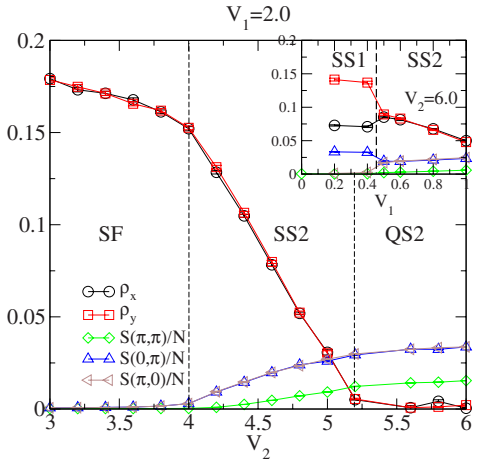

FIG. 4. (Color online) Ground state order parameters of a 28×28 lattice at $\rho=0.75$ for different V_2. Inset shows the first order phase transition at $V_2=6.0$.

same model but with the NNN hopping t' included also observes the QS2 and SS2 phases. Our result indicates that t' plays no significant role in the stabilization of both QS2 and SS2 phases, which instead is a direct consequence of competition between V_1 and V_2 interactions. Furthermore, contrary to our findings, Chen *et al.* observed a crossover from SS1 to SS2. Whether it arises from t' is still unclear.

Moving down from the cross along the dashed line in Fig. 1, the width of the QS2 plateau shrinks as V_2 decreases. When $V_2\approx5.2$, the QS2 phase disappears and the ground state changes continuously to the SS2. Figure 4 shows how ρ_s and $S(\mathbf{Q}_0)/N$ change as functions of V_2 at $V_1=2.0$. By reducing the NNN repulsion, the system gains kinetic energy that favors superfluidity and softens the solid structure at the same time. Consequently, QS2 continuously changes to SS2 and eventually to SF at $V_2=4.0$, where all peaks of $S(\mathbf{Q}_0)/N$ vanish simultaneously. Note that there is a large parameter range where SS2 is stabilized at this commensurate density $\rho=0.75$.

A more complicated situation arises for $V_1<1$, in which the NN repulsion is too weak to support the starlike structure against the striped one. Figure 1 shows the emergence of SS1 at small $V_1<1$ within the SS2 regime. The phase transition between SS1 and SS2 is again first order because of the different broken translational symmetries (inset of Fig. 4). For vanishing V_1, neither SS2 and QS2 is stabilized and the ground states are found to have striped ordering for all fillings, consistent with the previous findings.[3] In other words, the necessary condition for the appearance of the starlike quantum solid and supersolid is the competition between NN and NNN interactions.

To further investigate the effect of finite V_1, we plot in Fig. 5 the phase diagram of fixed $V_1=2$ with varying μ. The phase diagram is similar to the case of vanishing V_1 (see Ref. 3) except that two other phases, SS2 and QS2, emerge within the SS1 phase. Within this phase, by increasing μ (e.g., along the dashed line) such that ρ approaches 0.75, the starlike ordering becomes energetically more favorable than the striped ordering as discussed before and SS2 or QS2 is stabilized. Note that this happens only when $V_2>4$; otherwise, the SS1 state simply dissolves into the SF state upon increasing ρ. The emergence of SS2 and QS2 in the phase diagram reflects the interplay of NN and NNN interactions of the system.

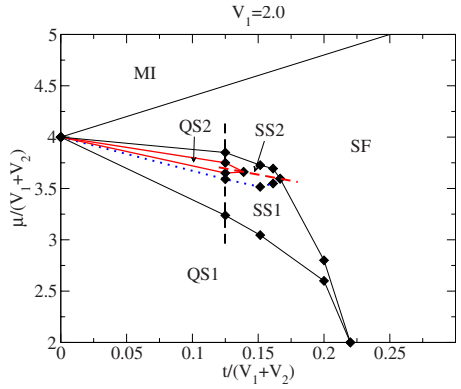

FIG. 5. (Color online) Phase diagram of μ vs t for fixed $V_1=2.0$. The lines are drawn to guide the eyes, with a dashed line (solid line) for first (second) order phase transitions. The change of order parameters along the black dotted line at $V_2=6.0$ is plotted in Fig. 2, while that along the red dottedline at fixed $\rho=0.75$ is displayed in Fig. 4. MI denotes the fully occupied Mott insulating phase.

Now let us present our results by VMC in support of the star solid QS2 and SS2 found in the QMC calculation. The wave function we used is the standard Jastrow wave function, which is defined as

$$|\Psi\rangle=\exp\left(-\sum_{i\neq j}v_{i,j}n_in_j\right)|\Phi_0\rangle, \tag{2}$$

where $|\Phi_0\rangle=(b_{k=0}^{\dagger})^N|0\rangle$ is the noninteracting superfluid wave function and N is the total number of bosons. In order to incorporate all kinds of phases in the same wave function, the pairwise potential $v_{i,j}$'s are independently optimized by the algorithm proposed by Capello *et al.*[12] To determine the phase diagram, we calculate the number of bosons in the zero momentum mode, the condensate, $N_{k=0}=b_{k=0}^{\dagger}b_{k=0}$, $S(\pi,0)$, and $S(\pi,\pi)$ for the optimized wave function. In Fig. 6(a), three order parameters are shown as a function of density for given $V_1=4$ and $V_2=6$. As density increases, the phase changes from SF to SS2 around the QS2 at $\rho=0.25$. With $\rho>0.28$, $S(\pi,0)$ vanishes and the system becomes a SS1 and a QS1 at $\rho=0.5$. This is consistent with the phase diagram (Fig. 1) obtained by QMC. In order to verify if the SS2 is thermodynamically stable, we show the boson density as a function of μ, which is calculated from the energy of adding an extra particle to the system $\mu=E(N+1)-E(N)$. Two plateaus are found at densities $\rho=0.25$ and 0.5, which correspond to QS2 and QS1, respectively. A positive slope around the plateau at $\rho=0.25$ indicates that the SS2 found is stable against phase separation. Although there are discrepancies in the position of the phase boundaries, the Jastrow wave function alone captures the essential features, and successfully generates all the observed phases in QMC.

In Fig. 7(a), we show the order parameters as a function

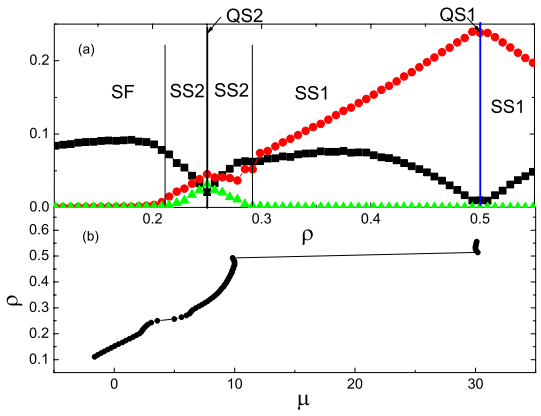

FIG. 6. (Color online) VMC results of (a) the condensate $N_{k=0}$ (square) and structure factor of wave vectors (π,π) (circle) and $(0,\pi)$ (triangle) as functions of density, and (b) boson density ρ as a function of the chemical potential. Here, V_1=4, V_2=6, and lattice size is 24×24.

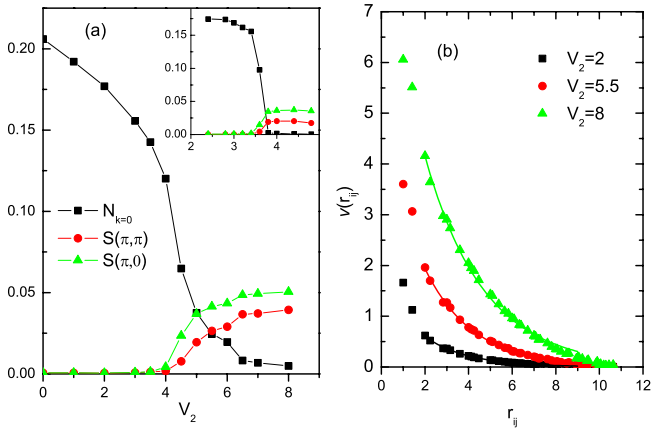

FIG. 7. (Color online) (a) VMC results of the condensate $N_{k=0}$, structure factor of wavevectors (π,π) and $(0,\pi)$ as functions of V_2 with V_1=4 and the boson density n=0.25. The inset shows the corresponding QMC data for comparison. Note that the black squares denote the superfluidity ρ_y in the QMC data. (b) The variational parameters $v_{i,j}$ vs r_{ij} for V_2=2, 5.5 and 8. The solid lines are the fitting functions of $Ae^{-r_{ij}/\xi}$. The lattice size is 24×24.

of V_2 with V_1=4 and ρ=0.25. The three phases found in Fig. 4 for V_2=2 are also observed here. The representative optimized variational parameters $v(r_{ij})$ for SF (V_2=2), SS2 (V_2=5.5) and QS2 (V_2=8) are shown in Fig. 7(b). The data ($r\geqslant2$) are fitted to an exponential form $Ae^{-r/\xi}$, with decay lengths ξ=2.0, 2.21, and 2.68 for SF, SS2, and QS2, respectively. The large value of $v(r_{ij})$ and ξ in the QS2 phase indicates the existence of a strong long-range repulsion between bosons, while the interaction is short range in the SS2 and SF phases accordingly.

In summary, we present numerical evidences for the appearance of a quantum solid, a supersolid phase with star pattern, and a striped supersolid at or around ρ=0.75 or 0.25. The competition between NN and NNN interactions is found to be important for the observation of both QS2 and SS2. A detailed study is given on the ground state phase diagrams by varying V_1 and V_2 as well as the chemical potential μ. The quantum phase transition between SS1 and SS2 appears to be first order because of the abrupt change of translational symmetry. Our VMC calculation also supports the QMC findings, and the simple Jastrow wave function alone is adequate to generate all the phases, consistent with the QMC calculations.

Note added. Recently, we notice that Chen *et al.* have updated their preprint with new results for larger L, showing that the transition between SS2 and SS1 is first order, consistent with our findings.

The authors thank M. F. Yang for fruitful discussions and acknowledge the support of the National Center for Theoretical Science. K.K.N. acknowledges financial support by the NSC (R.O.C.), Grants Nos. NSC 95-2112-M-029-010-MY2 and NSC 95-2110-M-029-004. Y.C.C. is supported by NSC 95-2112-M-029-003-MY3. Part of the calculation is supported by the National Center for High Performance Calculation (Taiwan).

[1] O. Penrose and L. Onsager, Phys. Rev. **104**, 576 (1956).
[2] A. F. Andreev and I. M. Lifshitz, Sov. Phys. JETP **29**, 1107 (1969); G. V. Chester, Phys. Rev. A **2**, 256 (1970); A. J. Leggett, Phys. Rev. Lett. **25**, 1543 (1970).
[3] G. G. Batrouni and R. T. Scalettar, G. G. Batrouni, R. T. Scalettar, G. Schmid, M. Troyer, and A. Dorueich, Phys. Rev. Lett. **84**, 1599 (2000); F. Hebert, G. G. Batrouni, R. T. Scalettar, G. Schmid, M. Troyer, and A. Dorneich, Phys. Rev. B **65**, 014513 (2001).
[4] P. Sengupta, L. P. Pryadko, F. Alet, M. Troyer, and G. Schmid, Phys. Rev. Lett. **94**, 207202 (2005).
[5] S. Wessel and M. Troyer, Phys. Rev. Lett. **95**, 127205 (2005); D. Heidarian and K. Damle, *ibid.* **95**, 127206 (2005); R. G. Melko, A. Paramekauti, A. A. Burkov, A. Vishwanath, D. N. Sheng, and L. Balents, *ibid.* **95**, 127207 (2005).
[6] K. K. Ng and T. K. Lee, Phys. Rev. Lett. **97**, 127204 (2006).
[7] N. Laflorencie and F. Mila, Phys. Rev. Lett. **99**, 027202 (2007).
[8] P. Sengupta and C. D. Batista, Phys. Rev. Lett. **98**, 227201 (2007).
[9] G. Schmid, S. Todo, M. Troyer, and A. Dorneich, Phys. Rev. Lett. **88**, 167208 (2002).
[10] Y. C. Chen, R. Melko, S. Wessel, and Y. J. Kao, Phys. Rev. B **77**, 014524 (2008).
[11] A. W. Sandvik, Phys. Rev. B **59**, R14157 (1999); **56**, 11678 (1997); O. F. Syljuåsen and A. W. Sandvik, Phys. Rev. E **66**, 046701 (2002).
[12] M. Capello, F. Becca, M. Fabrizio, and S. Sorella, Phys. Rev. Lett. **99**, 056402 (2007); S. Sorella, Phys. Rev. B **71**, 241103(R) (2005).